



HAL
open science

Control of high voltage direct current links with overall large-scale grid objectives

Leyla Arioua, Bogdan Marinescu, Eric Monmasson

► To cite this version:

Leyla Arioua, Bogdan Marinescu, Eric Monmasson. Control of high voltage direct current links with overall large-scale grid objectives. *IET Generation, Transmission and Distribution*, 2014, 8 (5), pp.945 - 956. 10.1049/iet-gtd.2013.0298 . hal-01421766

HAL Id: hal-01421766

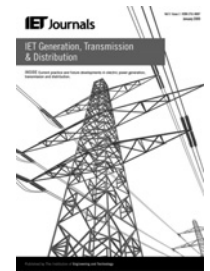
<https://hal.science/hal-01421766>

Submitted on 17 Mar 2020

HAL is a multi-disciplinary open access archive for the deposit and dissemination of scientific research documents, whether they are published or not. The documents may come from teaching and research institutions in France or abroad, or from public or private research centers.

L'archive ouverte pluridisciplinaire **HAL**, est destinée au dépôt et à la diffusion de documents scientifiques de niveau recherche, publiés ou non, émanant des établissements d'enseignement et de recherche français ou étrangers, des laboratoires publics ou privés.

Published in IET Generation, Transmission & Distribution
 Received on 29th April 2013
 Revised on 1st October 2013
 Accepted on 1st November 2013
 doi: 10.1049/iet-gtd.2013.0298



ISSN 1751-8687

Control of high voltage direct current links with overall large-scale grid objectives

Leyla Arioua^{1,2}, Bogdan Marinescu^{1,2}, Eric Monmasson³

¹R&D Division of Réseau de Transport d'Électricité de France, 78005 Versailles, France

²SATIE-CNRS Laboratory, Ecole Normale Supérieure de Cachan, 94235 Cachan cedex, France

³SATIE-CNRS Laboratory, Cergy-Pontoise University, site de Neuville 95031 Cergy-Pontoise cedex, France

E-mail: leyla.arioua@rte_france.com

Abstract: When a high voltage direct current (HVDC) link connects two distinct power systems, the latter are usually modelled by two infinite buses. However, in some context of use, the HVDC links are no longer separating two systems but they are embedded into meshed AC systems in parallel with other AC lines and interact with other elements of the power system. This led us to enhance the control objectives by considering stability requirements. In this context, the previous modeling assumption presents serious limitations. Instead, a more efficient control model is used. It is developed such that the concerned dynamics of the system are taken into account during the synthesis. It is shown how the controllers of the HVDC converters can be synthesised using the control model mentioned above such that global grid performances are ensured, in addition to the local objectives like power and DC voltage control. In order to avoid remote measures, an output feedback control which uses only local measures is developed. The new controller is tested in comparison with the standard vector control and a non-linear feedback linearisation control via simulation tests. The tests showed that the controller synthesised using the new control model contributes to a better coordination of the control actions and thus improve grid performances. In particular, the transient stability of the neighbour zone is a priori taken into account at the synthesis level.

1 Introduction

The high voltage direct current (HVDC) link is a mean of transmission of electric power based on high power electronics which offers an opportunity to enhance controllability, stability, and power transfer capability of AC transmission systems [1]. It was first used in power systems to interconnect asynchronous AC systems. The ends of the HVDC link are electrically independent one from each other and this avoids the propagation of perturbations (as short-circuits, loss of a power group, etc.) between the two AC grids. Many examples of asynchronous interconnections can be found, as it is the case of the England-France interconnection [2]. This separation between the two electric systems makes easy to design control laws for power electronic converters because the other dynamics of the power systems are not taken into account during the synthesis. However, HVDC links are increasingly used inside a same AC network in order to enhance the power transmission capacity at some points of the grid and meet the growing demand in terms of power exchange capacity. In this context, the HVDC link co-exists with other parallel AC lines and other elements as machines, injectors, etc. This is the case, for example, of the existing links as Caprivi link (Namibia), Kii Channel HVDC Project (Japan), Fenno-Skan (Finland-Sweden), Guizhou-Guangdong (China) [3], Kingsnorth HVDC Link (England) and the HVDC Pacific inter-tie [4] for which many studies as [5, 6]

were carried out. Note that some of these lines are of considerable length (about 950 km for Caprivi link). Some other projects of AC embedded DC lines of shorter length are underway in Europe as, for example France-Spain HVDC interconnection [7] of about 65 km.

Studies have shown, that the method of controlling HVDC converters have an impact on stability of the system in which the link is inserted [8–15]. The transient stability aspect is more stringent as the link is short and in parallel with AC lines. This led us to revise in this work the synthesis of the control laws of the HVDC converters in order to consider grid requirements, as the improvement of the transient stability, or, at least the non-deterioration of it. Several HVDC controller schemes based on various techniques have been proposed to enhance dynamic performances of power systems in case of HVDC operating in parallel with AC transmission lines. In [16] for example, the authors proposed a robust control scheme for a parallel AC/DC system. The paper describes a coordinated controller based on on-line identification of the power system parameters. A non-linear control strategy for HVDC converters based on remote information from generators was developed using the SIngle Machine Equivalent method [17]. In [18], an adaptive optimal control was developed using real time system-wide measurements. However, even these control methods show a positive impact on system stability and can be applied to large-scale power system, most of them need remote information that are not always available at the

HVDC converters or need the use of Wide-area measurement system as it is the case in [19, 20]. Our hypothesis in this paper is that no remote measure is available and we are looking for the best solution in this situation. Of course, in case of use of such remote signals, the behaviour of the control loop can be much improved. In other methods, the transient stability is considered as an a priori objective for the synthesis of coordinated controllers for HVDC. Thus, the whole AC system is considered in the control model [21, 22] but the effectiveness of these methods had not yet been studied in the case of large-scale power systems.

We focused in our work on the situation where only local measurements are used. For this purpose, a coordinated controller for HVDC converters is developed using a pole placement via an output feedback. The coordination of the control actions of the two converters contributes to generally improve the performances (better dynamics in nominal as well as in critical situations). However, in the particular situations of breakdown in communication between the two converters of the HVDC link, an emergency control is proposed. The latter is split into two parts, one for each converter and uses only local measurements. The controller synthesis is done in both cases (nominal and emergency) on the base of a ‘control model’ which is developed in order to capture dynamics that are relevant for the transient stability of the power system. However, the simplest control model used in power system is the so-called ‘machine on infinite bus’ used to tune the AVR for conventional generators [23]. In [24], a Thevenin equivalent of the AC system was used on each side of the DC link to take into account the rest of the system in order to improve the local performances of the HVDC controls. In our case and in order to capture the main ‘transient dynamics’, a richer control model which contains dynamic models of machines is used here. Only some generators of the system are retained in this model. These generators are those that most impact the transient stability. This strategy improves the way to consider ‘at the synthesis stage’ the neighbour zone even for ‘large-scale’ power systems.

The proposed control is tested in comparison with the standard vector control and the non-linear feedback linearisation control via simulations performed with Eurostag [25] and Simulink (SimPower Toolbox). The rest of the paper is organised as follows: in Section 2, a method for developing a control model for the power system in which the HVDC link is inserted is presented and followed by simulation tests. This control model is used in Section 3 to synthesise an output-feedback controller for HVDC converters. In Section 4, simulation results are presented to put in evidence the performances and the robustness of the proposed controller. Finally, in Section 5, an emergency control is proposed for the case of a breakdown in the communication system of the HVDC link.

2 Control model synthesis

2.1 Description of the 23-machines benchmark of France–Spain–Portugal network

A simplified representation of the France–Spain–Portugal zones introduced in [26] is used here as a benchmark. It consists of 23 machines as shown in Fig. 1. The system is represented by a detailed non-linear model including generators along with their regulations. Only the high voltage network (225 and 400 kV) is modelled. The

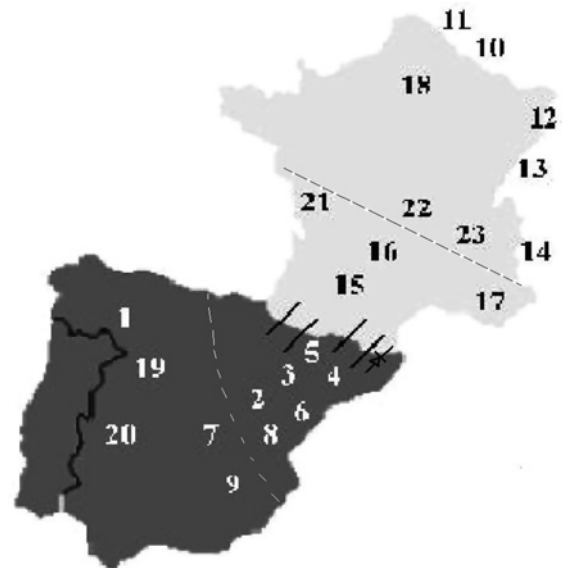


Fig. 1 France–Spain–Portugal interconnected systems

interconnection between France and Spain which consists of four AC lines is reinforced by adding a VSC-based HVDC link of 65 km length with a nominal active power of 1000 MW and a rated pole voltage of ± 320 kV.

2.2 Control objectives

The synthesis of the HVDC controller is done such that the global stability performances are ensured (i.e, the enhancement of transient stability or at least the non-deterioration of it) along with local ones (i.e, tracking of references for active power, reactive power and DC voltage).

2.3 Structure of the control model

The control model is composed of two parts: the AC power system (grid and machines) and the HVDC link (Fig. 2). In order to capture the dynamics which may deteriorate the transient stability of the overall power system, we retain in the control model ‘the most critical machines’, that is, those

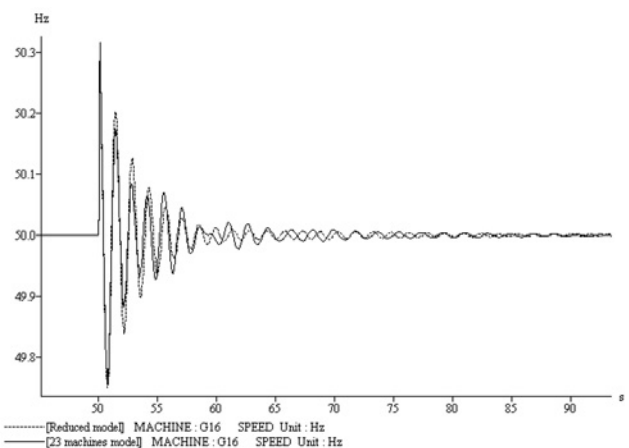


Fig. 2 Speed of G16 in the two cases of 23 machines and 4 machines models

which cause the system loss of synchronism after a severe perturbation. A transient stability margin of the power system is estimated by the Critical Clearing Time (CCT) which is defined as the maximal fault duration for which the system remains transiently stable [23]. The instability is then manifested by the loss of synchronism of a group of machines. The most critical of them are retained in the control model. The irrelevant topology of the electric network is also reduced.

2.4 Construction of the control model

2.4.1 Step 1: selection of the study area: The study area is the zone which is impacted by the HVDC link. More specifically, this corresponds to a neighbour zone of the DC interconnection of which transient stability depends on the HVDC dynamics. The extent of this zone is detected by standard stability studies usually run by TSOs. For our example, this zone is limited by the dotted line in Fig. 1.

2.4.2 Step 2: selection of critical machines: The strategy of machines selection is based on the computation of CCT at well-chosen points of the study area. As the study area, these points are determined by the same type of a priori stability study. To each case of fault, it is associated the first machine which loses synchronism and the corresponding CCT. The CCTs are next ordered in an ascending order and the η lowest values which are situated under a chosen level l are retained. Using this method, only η machines are retained. Several models can thus be obtained depending on the number of machines kept. It is obvious that the higher the number of machines kept is, the closer the control model is to the full one. Therefore, a trade-off must be achieved between the size of the control model and its performances (CCTs obtained from the reduced model close to the values obtained with the full model).

2.4.3 Step 3: network reduction: The topology is also reduced. More precisely, the buses to which the retained machines are connected are kept along with the end buses of the interconnections of interest (the HVDC link ones and the neighbour AC ones). The rest of the buses and branches are replaced by a WARD-PV method [27], that is, by equivalent impedances and injectors.

2.5 Modelling of the HVDC-VSC

In our study, a voltage-source converters (VSC) based HVDC is considered as in Fig. 3a. The converters are VSC employing IGBT power semiconductors, one operating as a rectifier and the other as an inverter. The two converters are connected through a DC cable. These converters have the ability to rapidly control the transmitted active power, and also to independently exchange reactive power with the AC system at each end. The high frequency switching operation of the power electronics is neglected and each converter can be considered as an ideal sinusoidal voltage source whose magnitude U_c and phase angle θ can be controlled (see [28]). The VSC-HVDC is thus modelled as two sources, each one in series with the converter transformer (see Fig. 3b where $\bar{U}_{c1} = U_{c1i} + jU_{c1j}$, $\bar{U}_{c2} = U_{c2i} + jU_{c2j}$ and θ_1, θ_2 are, respectively, the magnitudes and the phase angles of the voltage sources, P_1, P_2 , and, Q_1, Q_2 are, respectively, active and reactive powers exchanged with the power system and $X_{T,1}, X_{T,2}$ are the transformer reactances). In this model of HVDC, it is assumed that the DC voltage is kept close to its rated voltage, because its dynamic is much faster than the one of currents. Therefore, the losses of the converters are assumed constant, regardless of the current through the converters. They are represented as a constant active load [28]. This leads to

$$\begin{aligned} P_1 &= \left(U_1 \left(\sin\theta_1 U_{c1i} - \cos\theta_1 U_{c1j} \right) \right) / X_{T,1} \\ Q_1 &= \left(U_1^2 - U_1 \left(\cos\theta_1 U_{c1i} - \sin\theta_1 U_{c1j} \right) \right) / X_{T,1} \\ P_2 &= \left(U_2 \left(\sin\theta_2 U_{c2i} - \cos\theta_2 U_{c2j} \right) \right) / X_{T,2} \\ Q_2 &= \left(U_2^2 - U_2 \left(\cos\theta_2 U_{c2i} - \sin\theta_2 U_{c2j} \right) \right) / X_{T,2} \end{aligned} \quad (1)$$

In addition, note that $P_2 = -P_1$. The control variables can be expressed as follows

$$\begin{aligned} U_{c1i} &= U_{c1i0} + \Delta U_{c1i}, & U_{c1j} &= U_{c1j0} + \Delta U_{c1j} \\ U_{c2i} &= U_{c2i0} + \Delta U_{c2i}, & U_{c2j} &= U_{c2j0} + \Delta U_{c2j} \end{aligned} \quad (2)$$

2.6 Validation of the control model

Table 1 shows the machines kept for this study. The CCT threshold has been fixed to 300 ms. The resulting control

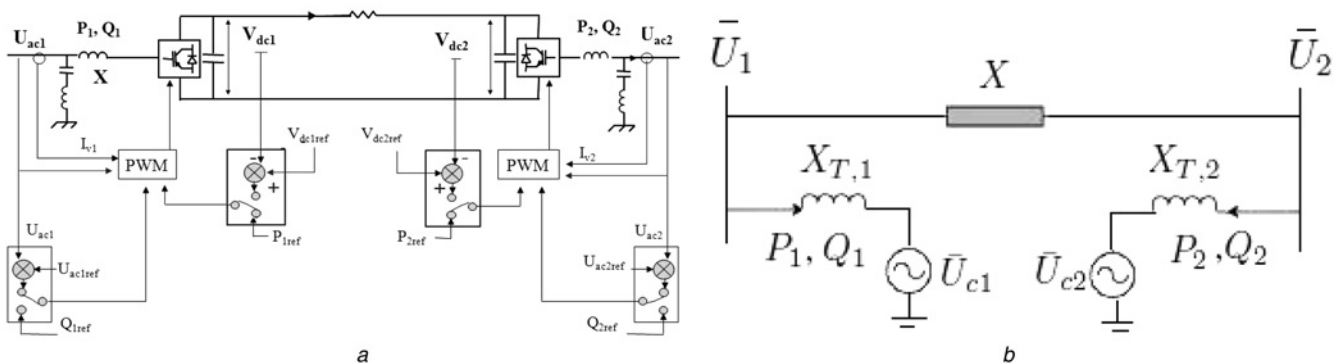


Fig. 3 VSC-HVDC link
a Scheme of full VSC-HVDC
b Simplified model of VSC-HVDC

Table 1 Selected critical machines

Gen, Fr	CCT, ms	Gen, Sp	CCT, ms
G16	64	G2	178
G15	203	G8	179
G17	205	G5	214
G21	280	G6	235

Table 2 Comparison of CCTs [ms] obtained for different models

	23Gen	8Gen	4Gen
fault 1	170	177	180
fault 2	239	273	268
fault 3	176	174	203
fault 4	220	290	303

models are validated by comparing the CCTs they provide, with the ones obtained with the full 23-machines model. The retained control model is the one that ensure the best trade-off between its dimension and its performances (see Section 2.4.2). As it is shown in Table 2, the 4-machine model seems to be the most appropriate control model. The Fig. 3 shows the speed responses of the generator G16 to a fault in two cases of 4-machine and 23-machine models.

3 Synthesis of the control law

3.1 Structure of the controller

To avoid the use of remote variables (e.g., machines speed, angles, ...), an output feedback law is used. Only variables available at converter stations are used. In addition, only one centralised and coordinated controller is developed for both converters (see Fig. 4a). For the work reported here, the controller has been developed using the linear approximation of the control model around an equilibrium point. The latter should be any point which satisfies the usual linearisation conditions, that is, which avoids variable limitations (like saturations, hysteresis,...) and singular operating conditions.

3.2 Linear approximation of the control model

Let the control model which includes the four machines and their regulations (AVRs and governors) be represented by

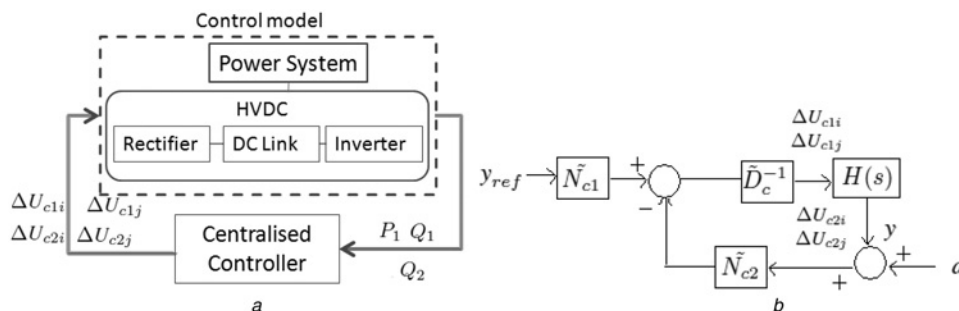


Fig. 4 HVDC controller

a Structure of the centralised controller
b 2DOF implementation of the controller

the non-linear differential and algebraic equations

$$\begin{aligned} \dot{x} &= f(x, U) \\ y &= g(x, U) \end{aligned} \quad (3)$$

where x represents the state variables (speeds, angles of machines, AVRs and governors variables...) of the 4-machine control model, U the control variables, y the outputs and let y_{ref} be the control references

$$\begin{aligned} U &= [U_{c1i}, U_{c1j}, U_{c2i}, U_{c2j}] \\ y &= [P_1, Q_1, Q_2] \\ y_{ref} &= [P_{ref1}, Q_{ref1}, Q_{ref2}] \end{aligned}$$

The linearisation of the system (3) around a given equilibrium point (x_0, U_0) is

$$\Sigma: \begin{cases} \Delta \dot{x} = A \Delta x + B \Delta U \\ \Delta y = C \Delta x \end{cases} \quad (4)$$

where $\Delta x = x - x_0$, $\Delta U = [\Delta U_{c1i}, \Delta U_{c1j}, \Delta U_{c2i}, \Delta U_{c2j}]$, $\Delta y = y - y_0$ and A, B, C are constant matrices.

Note that dedicated tools (like, e.g. Eurostag [25]), provide the linear model (4) for large-scale power systems.

3.3 Synthesis of a two-degrees-of-freedom controller

The synthesis is done with the linear approximation model given in (4). A two-degrees-of-freedom (2DOF) output-feedback controller (see Fig. 4b) has been developed. The methodology is briefly recalled here. The reader should refer to [29] for details.

3.3.1 Class of stabilising controller: Let $H(s)$ be the transfer matrix of Σ in (4). Let $(N_p(s), D_p(s))$, $(\tilde{D}_p(s), \tilde{N}_p(s))$ be respectively, left and right coprime factorisation of H :

$$H(s) = N_p(s)D_p(s)^{-1} = \tilde{D}_p(s)^{-1}\tilde{N}_p(s) \quad (5)$$

Now, let $X(s), Y(s), \tilde{X}(s)$ and $\tilde{Y}(s)$ be proper and stable transfer matrices selected such that

$$\begin{aligned} XN_p + YD_p &= I \\ \tilde{N}_p\tilde{X} + \tilde{D}_p\tilde{Y} &= I \end{aligned} \quad (6)$$

Then, the set of all 2DOF compensators, that stabilise Σ is given by

$$\text{Set}(\Sigma) = \tilde{D}_c^{-1} [\tilde{N}_{c1} \quad \tilde{N}_{c2}] \quad (7)$$

where

$$\begin{aligned} \tilde{D}_c &= Y - R\tilde{N}_p \\ \tilde{N}_{c2} &= X + R\tilde{D}_p \end{aligned} \quad (8)$$

and \tilde{N}_{c1} is arbitrary and R is such that

$$|(Y - R\tilde{N}_p)| \neq 0 \quad (9)$$

3.3.2 Computation of the doubly co-prime factorisation: The pairs (A, B) and (A, C) are stabilisable and detectable. Let the constant gain matrices K and L be such that

$$\begin{aligned} A_0 &= A - BK \\ \tilde{A}_0 &= A - LC \end{aligned} \quad (10)$$

where A_0 and \tilde{A}_0 are Hurwitz (i.e, their eigenvalues belong to the left half complex plane). Then the doubly co-prime factorisation of H is given by

$$\begin{aligned} \tilde{N}_p &= C(sI - \tilde{A}_0)^{-1} B \\ \tilde{D}_p &= I - C(sI - \tilde{A}_0)^{-1} L \\ N_p &= C(sI - A_0)^{-1} B \\ D_p &= I - K(sI - A_0)^{-1} B \end{aligned} \quad (11)$$

and the solutions of the Bézout equation (6) are

$$\begin{aligned} X &= K(sI - \tilde{A}_0)^{-1} L \\ Y &= I + K(sI - \tilde{A}_0)^{-1} B \\ \tilde{X} &= K(sI - A_0)^{-1} L \\ \tilde{Y} &= I + C(sI - A_0)^{-1} L \end{aligned} \quad (12)$$

The terms $N_p, D_p, \tilde{D}_p, \tilde{N}_p, X, Y, \tilde{X}$ and \tilde{Y} are proper and stable transfer matrices.

3.3.3 Controller implementation: The implementation of the controller is done according to (Fig. 4b) where the terms \tilde{D}_{c1} and \tilde{N}_{c2} are given by (8) and \tilde{N}_{c1} is a proper and stable matrix. The gain matrix K is determined using a linear quadratic (LQ) pole placement (see, e.g., [30]), in order to perform an ‘optimal eigenvalue assignment’ for A_0 (given by (10)) by minimising the quadratic cost function with output weighting

$$J = \int_0^{\infty} (\Delta U^T R \Delta U + \Delta y^T Q \Delta y) dt \quad (13)$$

where R and Q are positive weighting matrices such that $R = \text{diag}(10 \ 10 \ 10 \ 10)$ and $Q = \text{diag}(1 \ 1 \ 1)$. The optimal

gain K is then determined using the standard *lqr* routine of Control Toolbox of Matlab [31].

Note that since \tilde{A}_0 given by (10) and \tilde{A}_0^T have the same eigenvalues, the same method used to determine K , is applied to find L^T .

We have added the constraint $\tilde{D}_c(0) = 0$, to introduce an integral action in the controller to ensure tracking of references without steady-state error in addition to the constraint $\tilde{N}_{c1}(0) = \tilde{N}_{c2}(0)$.

The Input/Output transfer of closed loop is then given by

$$H_{y_{\text{ref}} \rightarrow y} = N_p (\tilde{D}_c D_p + \tilde{N}_{c2} N_p)^{-1} \tilde{N}_{c1} \quad (14)$$

4 Simulation tests

This section deals with performances and robustness of the proposed control. Simulation tests using Eurostag software [25] are performed in both the 23-machine benchmark model and a model of the full European power system (see Section 4.8).

4.1 Description of alternative existing controls

The new controller is compared with two other controllers. The first one is the standard vector controller (see for example [32]) which has a cascade structure with an inner loop more rapid than the outer one. The proportional and integral gains of this control are synthesised using standard criteria for electrical drives. The second method deals with the non-linear feedback linearisation control [33]. For the latter, instead of using the well known PI controller (as it is the case in the standard vector control), a more effective control law is developed based on the input-output feedback linearisation. The controller gains are chosen through a pole placement technique. The three controllers are tuned to satisfy almost the same performance specifications (the usual time setting for HVDC voltage and power control).

4.2 Local performances

The centralised controller synthesised using the 4-machines control model is tested on the 23-machine benchmark introduced in Section 2.1. An export of 1000 MW is considered from France to Spain via the HVDC link. To test local performances, a -0.1 p.u step is applied to the reference of the active power transmitted through the HVDC link (P_{ref}). Figs. 5a and b show the responses of active and reactive powers. A good tracking of the active power reference and a satisfying time constants for both responses are observed. Note that the overshoot in the reactive power response (Fig. 5b) is of limited magnitude.

4.3 Transient stability

Figs. 6a and c show the responses of active and reactive powers to a symmetrical short-circuit of 100 ms occurring near the converter 1 (French side) in the case of the 23-machine benchmark. It can be observed better dynamic responses with the new coordinated controller. Furthermore, a severe short-circuit of 250 ms duration (which is close to the CCT at this point (CCT = 260 ms)) is applied. Figs. 7a and c show that the transient

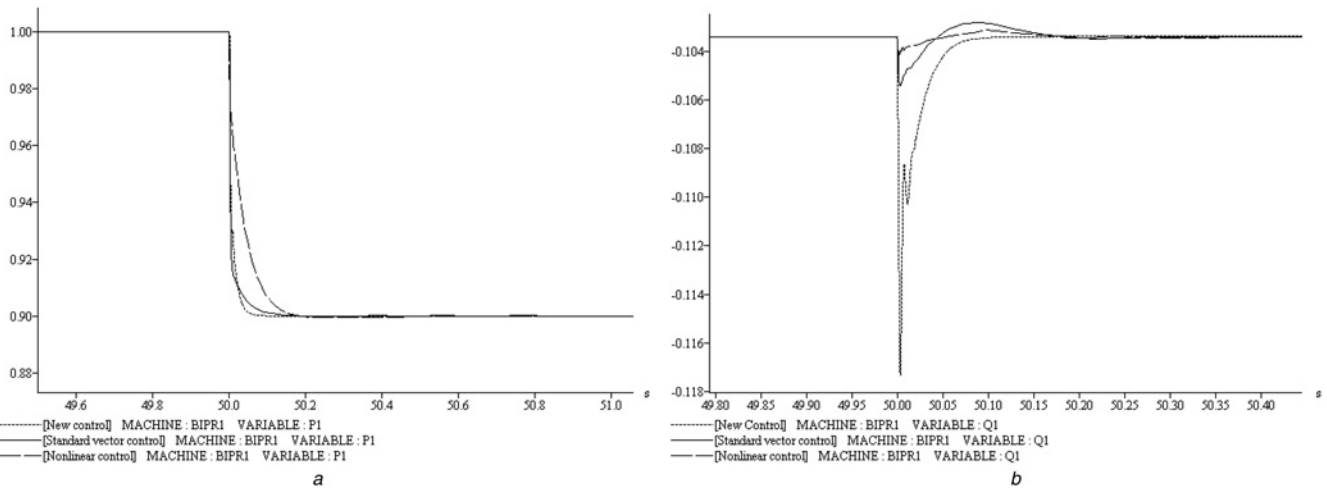


Fig. 5 Local performances of the new controller in case of power export
 a Response of P_1 to a -0.1 step in $Pref_1$ (p.u)
 b Response of Q_1 to a -0.1 step change in $Pref_1$ (p.u)

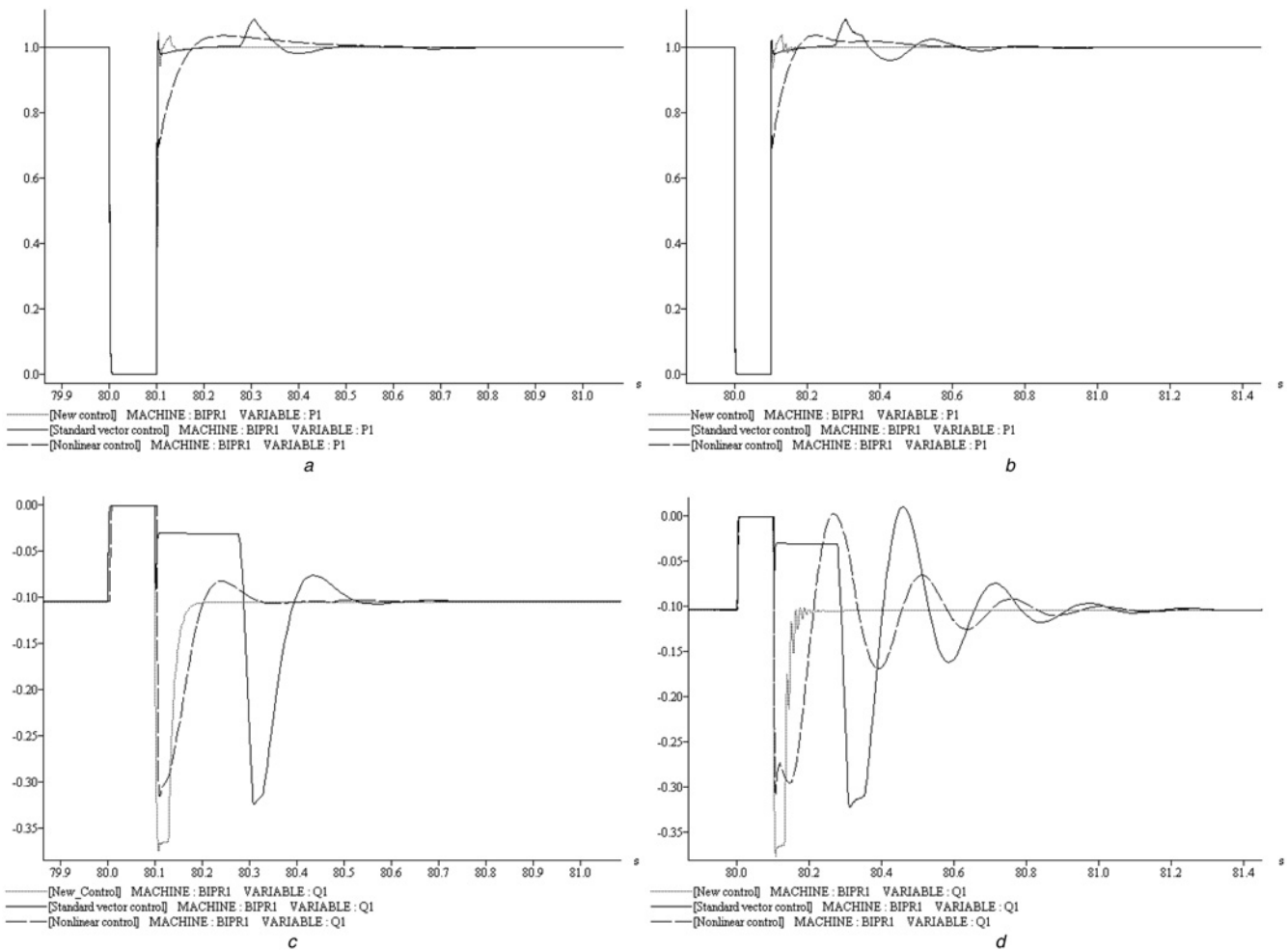


Fig. 6 Active and reactive power responses to a 100 ms short-circuit in case of power export
 a P_1 response to a 100 ms short-circuit (no time delay) (p.u)
 b P_1 response to a 100 ms short-circuit with 25 ms time delay (p.u)
 c Q_1 response to a 100 ms short-circuit (no time delay) (p.u)
 d Q_1 response to 100 a short-circuit with 25 ms time delay (p.u)

oscillations obtained with the new controller are more damped than the ones obtained with the standard vector control and the non-linear feedback linearisation control. In addition to the previous simulations and in order to

better investigate the transient stability, the critical clearing times obtained with the new controller were compared to the ones obtained when using the standard and the non-linear controls. The results are resumed in

Table 3 and confirm the improvement of transient stability in the case of the proposed controller.

Note also that the responses with the non-linear feedback linearisation controller are better than the ones with the standard vector controller thanks to the non-linear control strategy applied.

4.4 Dynamics without saturations

The simulation results presented above are performed using adequate saturation blocks and Anti-Windup filters for the PI blocks of the controllers for both control solutions, the proposed one and the standard one. This is the normal operation situation. However, Fig. 8, shows the current response (rectifier side) to a 4 ms short-circuit in the cases of the 23-machine benchmark without any saturation to better investigate the differences between the dynamics of the two controllers. It can be seen that the new controller generates signals of significantly less amplitude and overshoots than the ones obtained with the standard control. This leads to less severe saturations in operation. The improved behaviour put into evidence by the tests presented above can also be seen as a consequence of this.

4.5 A posteriori validation of the control model

In Section 2.4, an approach of machines selection has been developed and a trade-off between the size of the control model and its accuracy allowed us choosing the four machines control model. To check this choice, a posteriori validation have been done. In fact, CCTs have been computed for the closed loop obtained with regulators synthesised using control models of 2, 4 and 8 machines respectively (see Table 4). It can be seen that the CCTs obtained for the 4-machines and 8-machines cases are very close, which confirm the choice of keeping in the control model only the four most critical machines.

4.6 Robustness tests

4.6.1 Robustness against variation of the operating point: Since the synthesis of proposed controller was done using the linearised model, tests of robustness of performances against the variation of the operating point are necessary. So, a new load flow scenario is considered for the simulations. 600 MW are now imported from Spain to France. Note that the same controllers as before are used, i.e., the ones synthesised using the export situation. Figs. 9a

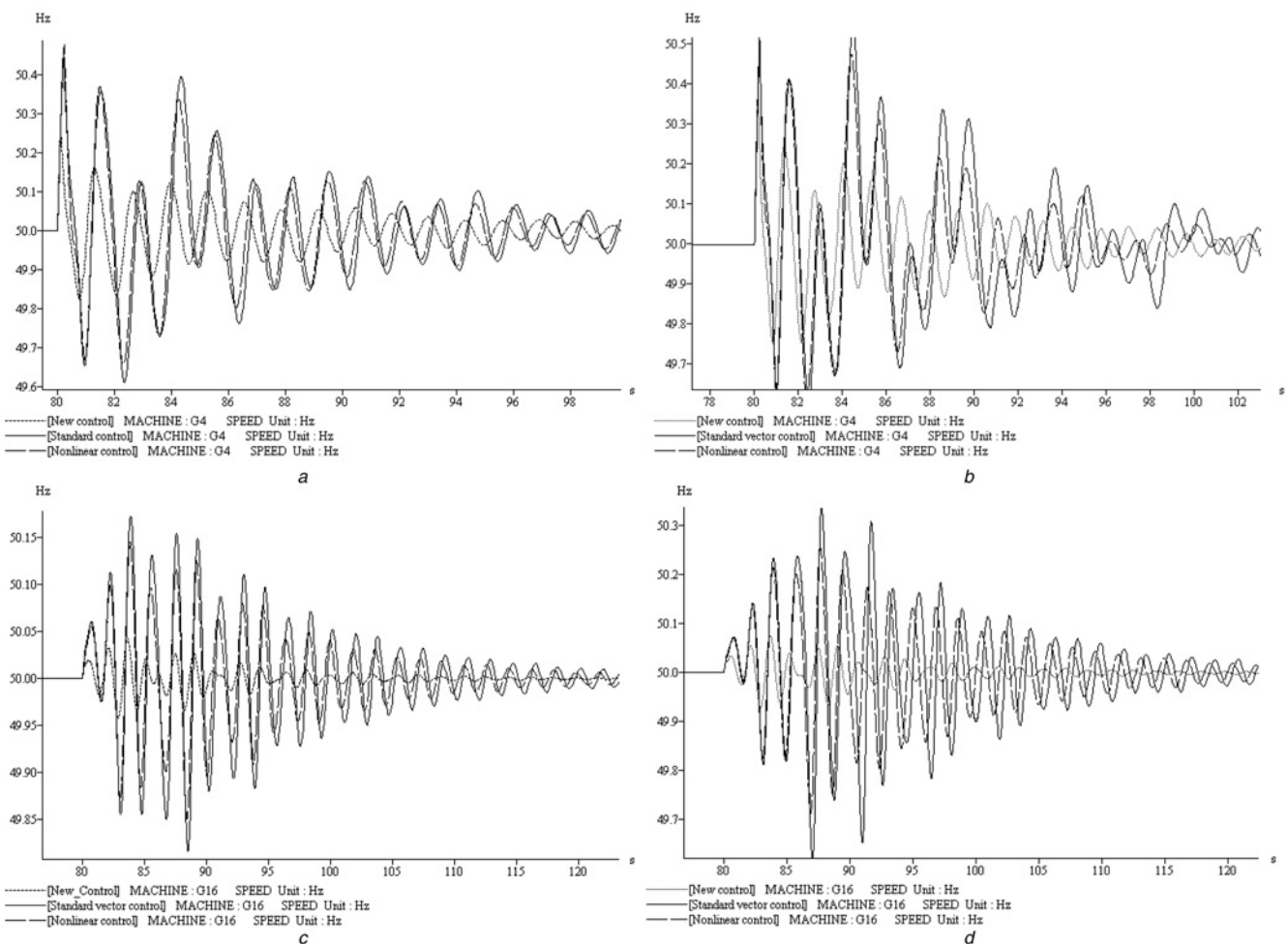


Fig. 7 Responses of the system to a 250 ms short-circuit in case of power export

- a Speed response of G4 (no time delay)(Hz)
- b Speed response of G4 with 25 ms time delay (Hz)
- c Speed response of G16 (no time delay)(Hz)
- d Speed response of G16 with 25 ms time delay (Hz)

Table 3 Critical clearing time validation of the new controller

Fault simulated	Standard controller CCT, ms	Non-linear controller CCT, ms	New controller CCT, ms
Asco1	158	164	175
Bescano	223	231	256
Stlog	260	268	296
Vic	240	243	267
Vandell1	165	170	180

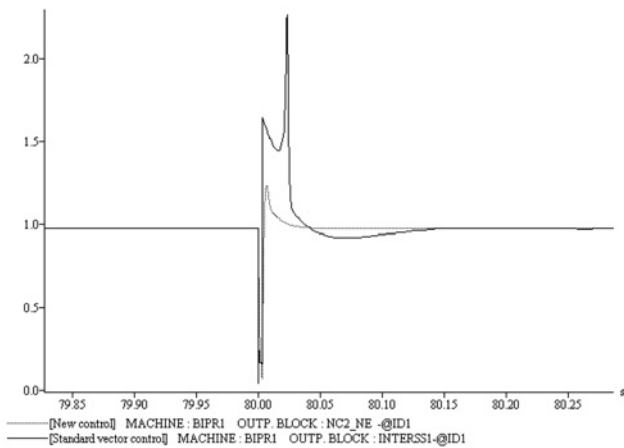


Fig. 8 Current response of current to a short-circuit in case of power export (p.u)

Table 4 CCT validation for different controllers [ms]

Fault near:	8 machines	4 machines	2-machines
Asco1	175	173–174	170
Bescano	256	254	220
Baixas	380	348	312
Stlog	297	295	258

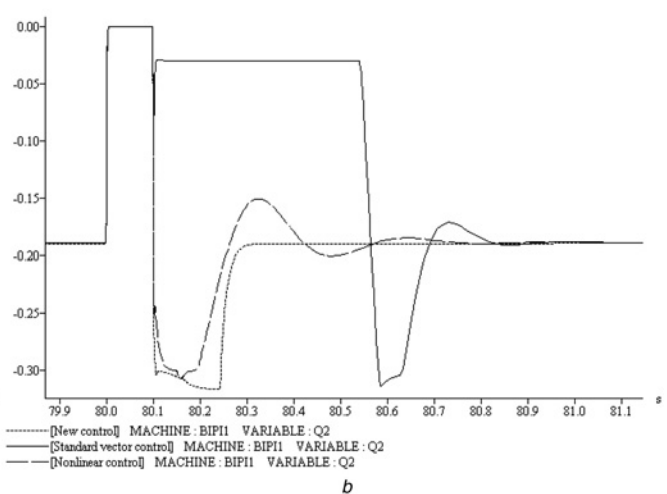
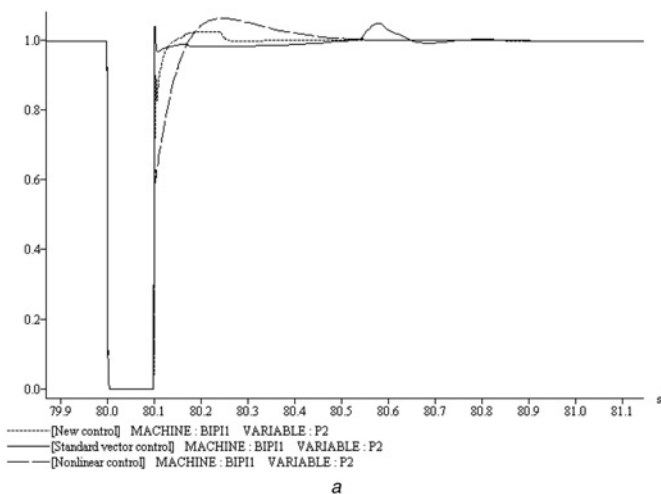


Fig. 9 Responses to a short-circuit in case of 600 MW power import

a P_2 response to a 100 ms short-circuit (p.u)
 b Q_2 response to a 100 ms short-circuit (p.u)

and b , are the active power and reactive power responses to 100 ms short-circuit applied near the converter 2 (Spanish side). Both are comparable with the ones obtained when the export scenario is used (Figs. 6a and c). Moreover, in this situation also, the responses are better than the ones obtained with the standard and non-linear controllers. This confirm the good robustness of the performances of the proposed controller against variation of operating conditions.

4.6.2 Robustness against transmission time delays:

The control law synthesis presented in Section 3 was done in the case of ideal transmission, that is, no time delay on measures and controls. In practice, some transmission delay might exist. Thus, we have performed some tests to investigate the robustness of the new controller against such time delays. We have observed that for a 100 ms time delay in the measure of the active power, the responses are not really impacted. However, for time delay of 25 ms and more in the measures of reactive powers, the effects of the time delay start to be notable, especially for the standard vector control and non-linear feedback linearisation control. Figs. 6b and d, show the responses of active and reactive powers when a 100 ms short-circuit fault occurs near the converter 1 and with a time-delay of 25 ms in reactive power measures. It can be observed that even there is a time delay, the proposed controller still maintain its performances, in comparison with the standard vector control and non-linear feedback linearisation control. In addition, when a 250 ms short-circuit is applied, Figs. 7b and d show, as for the case without delay, that the speed responses of the machines G4 and G16 with the proposed controller are more damped comparing to the ones obtained with the standard and non-linear controls. The delay margin with the proposed control is of approximately 45 ms. We conclude that the proposed controller is more robust against transmission time delay in comparison with the standard and non-linear controllers. However, for delays greater than a certain threshold, it would be unavoidable to make a synthesis taking into account the time-delays as it is the case for example in [19] or using a predictive control to ensure time-delay compensation. Note that certain predictive

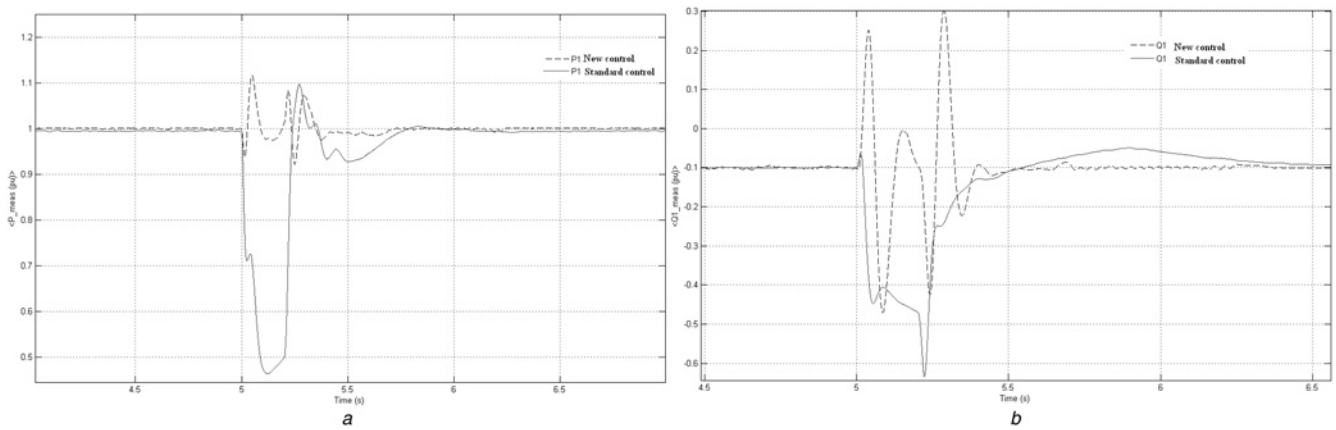


Fig. 10 Responses to a short-circuit in case of detailed VSC HVDC

a Active power transmitted
b Reactive power exchanged at converter 1

control methodologies are based on the ‘separation principle’ for which the regulator synthesised for the nominal system (i. e, without delays) is complemented by a predictor as it is the case in [34]. This issue is not treated in the present paper.

4.7 Detailed HVDC-VSC tests

In order to validate our approach when a detailed model of HVDC is considered, a regulator synthesised using a 2-machines control model is tested using the HVDC-VSC

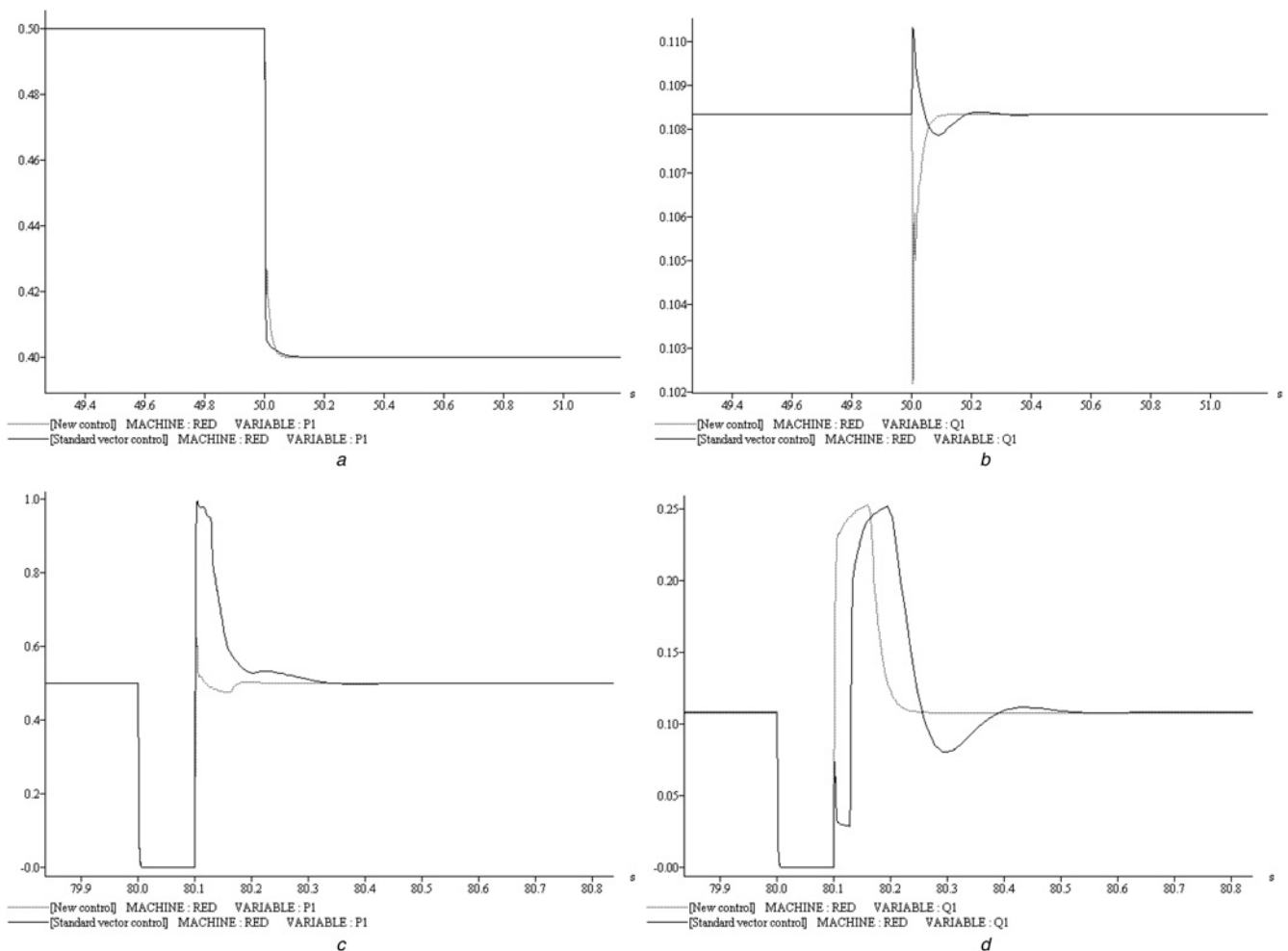


Fig. 11 Case of the full European power system

a P_1 responses to a -0.1 pu step in active power
b Q_1 response to -0.1 pu step in active power
c P_1 response to a 100 ms short-circuit (p.u)
d Q_1 response to a 100 ms short-circuit (p.u)

model of SimPower toolbox. A fault is applied near converter 1 and a comparison is done between the two case of standard controller and new one. Figs. 10a and b show the responses of active and reactive powers. It can be observed better dynamic responses in the case of the centralised controller comparing with the standard control.

4.8 Tests on the real European power system

To further validate the proposed HVDC controller and to bring out the control performances of the new coordinated controller, non-linear simulations were performed on the detailed non-linear model of the real European power system. This model is currently used by TSO's for dynamic analysis of the European interconnected system. It consists of 1121 generators along with their regulations, 7625 nodes, 10 404 lines, 2550 transformers and 458 GVA global apparent power. As in the benchmark used in previous sections, the interconnection between France and Spain is reinforced by adding an HVDC link of 1000 MW capacity. This link exports 0.5 pu from France to Spain. Fig. 11 shows the dynamic responses in case of the real European power system model for the two kinds of scenarios. The first one consists of a -0.1 step pu on the active power reference (Figs. 11a and b). For the second scenario, a 100 ms short-circuit is applied near the French station of the HVDC link Figs. 11c and d. As for the benchmark case, the responses show better performances comparing to the standard vector control.

5 Emergency control

The improvement of the transient stability and local performances is partially due to the coordinated structure of the proposed controller. Indeed, this controller uses measurements for both converters as shown in Fig. 4a. However, in the critical case of a breakdown in the communication, the new regulator cannot be used in its nominal form. In fact, in this case, the real-time information is available only at each converter (i.e., active power, reactive powers and voltages) but without the possibility to use them together as in the nominal operation. Thus, one converter will control the power flow (rectifier) and the second one will maintain the DC voltage (inverter). In what follows, we analyse the alternative to better preserve the coordinated nature of the proposed control under the constraints imposed above on the measurements. Three emergency control approaches can be considered:

5.1 Approach 1

For this first approach, the cross-terms in the transfer matrix of Σ in (4) are neglected. This is equivalent to consider a priori that the two HVDC converters don't interact. The controller is then synthesised based on the decoupled model of the system. Unfortunately, this assumption is not valid when the HVDC is used in the new context grid mentioned in Section 1 and tests done have shown that this approach cannot be used in case of emergency control. Note that this assumption is also used for the vector control for which the two converters are considered independently.

5.2 Approach 2

For the second approach cross-terms of the controller synthesised based on the whole coupled control model are neglected. Let G be the controller transfer function, that is, $\Delta U = G\Delta y$. G can be partitioned as

$$\begin{pmatrix} \Delta U_1 \\ \Delta U_2 \end{pmatrix} = \begin{pmatrix} G_{11} & G_{12} \\ G_{21} & G_{22} \end{pmatrix} \begin{pmatrix} \Delta y_1 \\ \Delta y_2 \end{pmatrix} \quad (15)$$

where

$$\Delta U_1 = \begin{pmatrix} \Delta U_{c1i} \\ \Delta U_{c1j} \end{pmatrix}, \quad \Delta U_2 = \begin{pmatrix} \Delta U_{c2i} \\ \Delta U_{c2j} \end{pmatrix}$$

and

$$\Delta y_1 = \begin{pmatrix} \Delta P_1 \\ \Delta Q_1 \end{pmatrix}, \quad \Delta y_2 = (\Delta Q_2)$$

It has been observed in practice that

$$\begin{aligned} \|G_{11}\|_2 > 10 \cdot \|G_{12}\|_2 \\ \|G_{22}\|_2 > 10 \cdot \|G_{21}\|_2 \end{aligned} \quad (16)$$

The terms G_{12} and G_{21} can thus be neglected.

5.3 Approach 3

The third approach consists in tuning the parameters of an a priori given structure of the controller (see, for example, [35]). For our case, a diagonal structure should be imposed to the regulator. This is, in general, a more difficult task (than approaches 1 and 2) and will be investigated in a future work.

5.4 Decoupled structure tests

Table 5 shows a comparison between the CCTs obtained with the two structures, the centralised one and the approach 2. These CCTs are better in case of the new centralised controller. In addition, tests were conducted when a fault occurs near the HVDC link to illustrate the difference between the centralised controller and the decoupled one (approach 2). Figs. 12a and b show better active and reactive power responses in case of the centralised controller. However, the responses obtained with the decoupled controller are acceptable.

6 Conclusion

A new approach for synthesising the converters controllers of HVDC link has been proposed. It is based on the coordination

Table 5 Critical clearing time in cases of centralised and decoupled structure

Fault occurred near:	Centralised controller CCT, ms	Decoupled controller CCT, ms
Stlog	297	293
Vandell1	180	179
Vic	269	258
Bescano	256	246

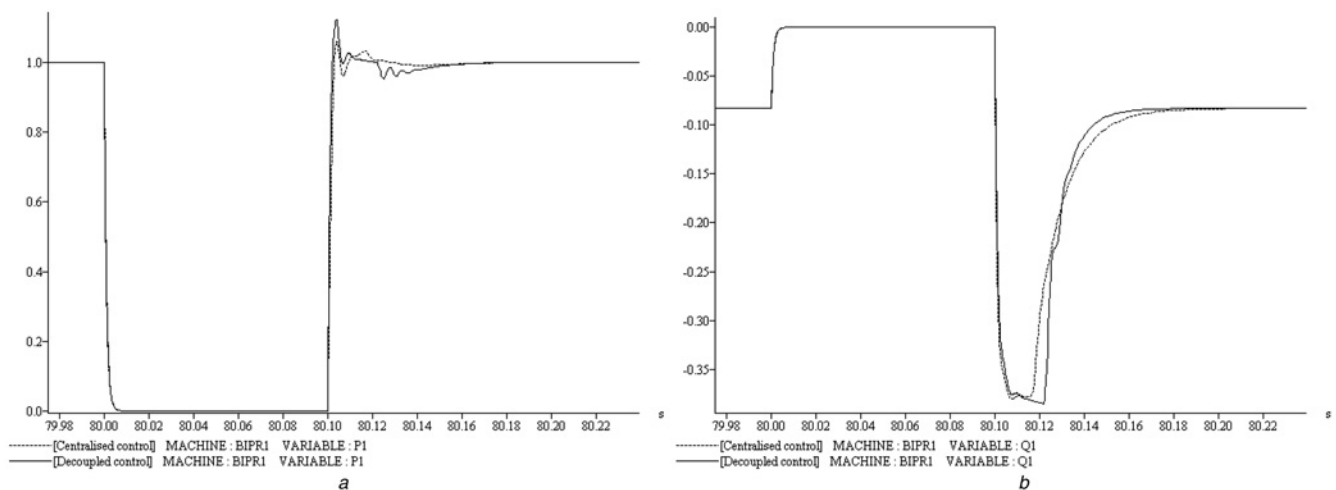


Fig. 12 Responses to a short-circuit (centralized and decoupled controller)

a P_1 response to a 100 ms short-circuit (p.u)

b Q_1 response to a 100 ms short-circuit (p.u)

of the control actions of the two converters and the use of a new control model which captures the important grid dynamics. As a consequence, overall objectives are ensured in addition to local performances. This contributes to a better insertion of this kind of devices in a power system. In particular, in this way the impact of the HVDC link on the transient stability of the neighbour zone is enhanced.

This new control framework is flexible and opens several perspectives:

- other control laws, like, for example, non-linear control, can be envisaged.
- the synthesis of the emergency controller can be refined with approach 3 (as mentioned in Section 5)
- small-signal stability objectives may be tracked within the same framework.

The use of the control model mentioned above is the key point to improve the performances since it provides the way to a priori (i.e., during the control synthesis process) take into account the main interactions of the system. This advantage will also be used in the future works to coordinate the control of several close HVDC links among each others and with the other neighbour actuators of the power system. Also, as mentioned before, more effective and optimal control methods can be used in this framework for both of the nominal and emergency levels and this will be treated in the forthcoming publications.

7 Acknowledgment

The authors would like to thank Dr. Alexandre Parisot, head of Integration of New Technology division (INT) of RTE for helpful suggestions and remarks.

8 References

- 1 Hingorani, G.N., Gyugyi, L.: 'Understanding FACTS: concepts and technology of exible AC transmission systems' (IEEE Press, Piscataway, 2000)
- 2 Goodrich, F., Andersen, B.: 'The 2000 MW HVDC link between England and France', *Power Eng. J.*, 1987, 1, (2), pp. 69–74
- 3 Mao, X.M., Zhang, Y., Guan, L., Wu, X.C.: 'Coordinated control of interarea oscillation in the China Southern power grid', *IEEE Trans. Power Syst.*, 2006, 21, (2), pp. 845–852

- 4 Litzemberger, W., Lips, P.: 'Pacific HVDC intertie', *Power Energy Mag. IEEE.*, 2007, 5, (2), pp. 45–51
- 5 Hammad, A., Minghetti, R., Hasler, J.P., Eicher, P.A., Bunch, R., Goldsworthy, D.: 'Controls modelling and verification for the Pacific Intertie HVDC 4-terminal scheme', *IEEE Trans. Power Deliv.*, 1993, 8, (1), pp. 367–375
- 6 Cresap, R.L., Scott, D.N., Mittelstadt, W.A., *et al.*: 'Operating experience with modulation of the Pacific HVDC intertie', *IEEE Trans. Power Appar. Syst.*, 1978, 97, (4), pp. 1053–1057
- 7 <http://www.inelfe.eu/>, INELFE Consortium
- 8 Hauer, J.F.: 'Robustness issues in stability control of large electric power systems'. Proc. 32nd IEEE Conf. on Decision and Control, 1993, pp. 2329–2334
- 9 Vovos, N.A., Galanos, G.D.: 'Enhancement of the transient stability of integrated AC/DC systems using active and reactive power modulation', *IEEE Power Eng. Rev.*, 1985, 5, (7), pp. 33–34
- 10 Smed, T., Andersson, G.: 'Utilizing HVDC to damp power oscillations', *IEEE Trans. Power Deliv.*, 1993, 8, (2), pp. 620–627
- 11 Hammad, A.E., Gagnon, J., McCallum, D.: 'Improving the dynamic performance of a complex AC/DC system by HVDC control modifications', *IEEE Trans. Power Deliv.*, 1990, 5, (4), pp. 1934–1943
- 12 Shun, F.L., Muhamad, R., Srivastava, K., Cole, S., Hertem, D.V., Belmans, R.: 'Influence of VSC HVDC on transient stability: Case study of the Belgian grid'. Proc. IEEE Power and Energy Society General Meeting, 25–29 July 2010, pp. 1–7
- 13 Taylor, C.W., Lefebvre, S.: 'HVDC controls for system dynamic performance', *IEEE Trans. Power Syst.*, 1991, 6, (2), pp. 743–752
- 14 Latorre, H.F., Ghandhari, M., Söder, L.: 'Control of a VSC-HVDC operating in parallel with AC transmission lines'. Proc. Transmission and Distribution Conf. and Exposition IEEE, Latin America, 2006, pp. 1–5
- 15 Henry, S., Despouys, O., Adapa, R., *et al.*: 'Influence of embedded HVDC transmission on system security and AC network performance'. Cigré, 2013
- 16 To, K., David, A., Hammad, A.: 'A robust co-ordinated control scheme for HVDC transmission with parallel AC systems', *IEEE Trans. Power Deliv.*, 1994, 9, (3), pp. 1710–1716
- 17 Latorre, H., Ghandhari, M.: 'Improvement of power system stability by using a VSC-HVDC', *Int. J. Electr. Power Energy Syst.*, 2011, 33, (2), pp. 332–339
- 18 Rostamkolai, N., Phadke, A.G., Long, W.F., Thorp, J.S.: 'An adaptive optimal control strategy for dynamic stability enhancement of AC/DC power systems', *IEEE Trans. Power Syst.*, 1988, 3, (3), pp. 1139–1145
- 19 Li, Y., Rehtanz, C., Yang, D., Rüberg, S., Häger, U.: 'Robust high-voltage direct current stabilising control using wide-area measurement and taking transmission time delay into consideration', *IET Gener. Transm. Distrib.*, 2011, 5, (3), pp. 289–297
- 20 Mao, X.M., Zhang, Y., Guan, L., Wu, X.C., Zhang, M.: 'Improving power system dynamic performance using wide-area high-voltage direct current damping control', *IET Gener. Transm. Distrib.*, 2008, 2, (2), pp. 245–251

- 21 Hu, Z., Mao, C., Lu, J.: 'Improvement of transient stability in AC system by HVDC Light'. Proc. Transmission and Distribution Conf. and Exhibition IEEE: Asia and Pacific, Dalian, 2005, pp. 1–5
- 22 Mao, C., Hu, Z., Lu, J., Chang, D., Fan, S.: 'Application of an optimal coordinated control strategy to VSC HVDC'. Proc. Power Systems Conf. and Exposition IEEE, Atlanta, 2006, pp. 2141–2145
- 23 Kundur, P.: 'Power stability and control' (McGraw-Hill, New York, 1994)
- 24 Lefebvre, S., Saad, M., Hurteau, R.: 'Adaptive control for HVDC power transmission systems', *IEEE Trans. Power Appar. Syst.*, 1985, **PAS-100**, (9), pp. 2329–2335
- 25 Meyer, B., Stubbe, M.: 'EUROSTAG, a single tool for power system simulation', *Trans. Distrib. Int.*, 1992, **3**, (1), pp. 41–52
- 26 Ramaswamy, G.N., Verghese, G.C., Rouco, L., Vialas, C., Demarco, C.L.: 'Synchrony, aggregation and multi-area eigenanalysis', *IEEE Trans. Power Syst.*, 1995, **10**, (4), pp. 1986–1993
- 27 Baldwin, T.L., Mili, L., Phadke, A.G.: 'Dynamic Ward equivalents for transient stability analysis', *IEEE Trans. Power Syst.*, 1994, **9**, (1), pp. 59–67
- 28 Latorre, H.F., Ghandhari, M., Söder, L.: 'Active and reactive power control of a VSC-HVDC', *Electr. Power Syst. Res.*, 2008, **78**, (10), pp. 1756–1763
- 29 Vidyasagar, M.: 'Control system synthesis: a factorization approach' (M.I.T.Press, Massachusetts, 1985)
- 30 Kwakernaak, H., Sivan, R.: 'Linear optimal control systems' (John Wiley, New York, 1972)
- 31 Guide, G.S.: 'Control System Toolbox', 2000
- 32 Li, S., Haskew, T.A., Xu, L.: 'Control of HVDC light system using conventional and direct current vector control approaches', *IEEE Trans. Power Electr.*, 2010, **25**, (12), pp. 3106–3118
- 33 Ruan, S.Y., Li, G.J., Peng, L., Sun, Y.Z., Lie, T.T.: 'A nonlinear control for enhancing HVDC light transmission system stability', *Int. J. Electr. Power Energy Syst.*, 2007, **29**, (7), pp. 565–570
- 34 Marinescu, B., Bourlès, H.: 'Robust state-predictive control with separation property: A reduced-state design for control systems with non-equal time delays', *Automatica*, 2000, **36**, (4), pp. 555–562
- 35 Erwin, R.S., Sparks, A.G., Bernstein, D.S.: 'Fixed-structure robust controller synthesis via decentralized static Output-Feedback', *Int. J. Robust Nonlinear Control.*, 1998, **8**, pp. 499–522